LANGMUIR

Editors' Choice

pubs.acs.org/Langmuir

Article

Dual-Mode Patterns Enabled by Photofluidization of an Azobenzene-Containing Linear Liquid Crystal Copolymer

Feng Pan, Yaoqing Feng, Yuyao Qian, Lang Qin,* and Yanlei Yu*

Cite This: *Langmuir* 2024, 40, 11766−11774

Read Online

ACCESS | Metrics & More | Article Recommendations | Supporting Information

ABSTRACT: Creating dual-mode patterns in the same area of the material is an advanced method to increase the dimension of information storage, improve the level of encryption security, and promote the development of encoding technology. However, in situ, different patterns may lead to serious mutual interference in the process of manufacturing and usage. New materials and patterning techniques are essential for the advancement of noninterfering dual-mode patterns. Herein, noninterfering dual-mode patterns are demonstrated by combining the structural color and chromatic polarization, which is designed with an azobenzene-containing linear liquid crystal copolymer featuring a photofluidization effect. On the one hand, structural color patterns are imprinted via silicon templates with periodic microstructures after a UV-light-induced local transition of the polymer surface from a glassy to rubbery state. On the other hand, different polarization patterns based on the local photoinduced orientation of mesogens are created within the photofluidized region by the Weigert effect. Especially, the secondary imprinting is used to eliminate the partial damage to the structural color patterns during writing of the polarization patterns, thus obtaining dual-mode patterns without interference. This study provides a blueprint for the creation of advanced materials and sophisticated photopatterning techniques with potential cross-industry applications.

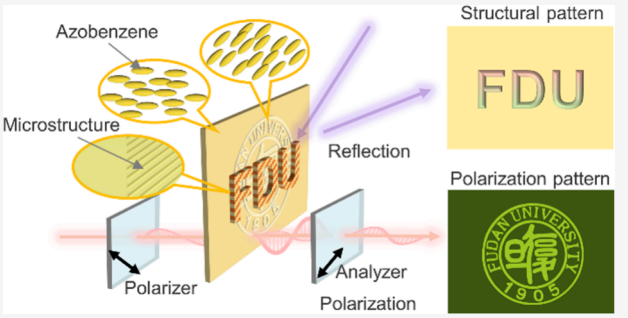

INTRODUCTION

Information storage and security are subjects of widespread global concern. To address this issue, researchers have developed numerous optical materials, such as photonic crystals,[1−4] stimulus-responsive materials,[5,6] and luminescent materials,[7−9] used for authenticating banknotes, valuable products, important documents, and so on. Patterned polymer materials are widely applied in encryption and information storage, which influence the propagation of light and modulate signals through the interactions with light.[10−16] Self-assembly in polymer materials enables micro/nanoscale ordered structures and controlled designs for patterning. This process can be triggered via various methods such as block copolymer phase separation, supramolecular interactions, or template-assisted assembly.[17] For example, the introduction of periodic structures via self-assembly into these materials leads to the creation of photonic crystals, which allow the regulation of light propagation through their photonic band gaps.[18] Compared with the single-mode patterns, dual-mode patterns typically possess two different patterns in the same regions of the polymers, which are capable of independent storage and reading.[19,20] Notably, the combination of structural color patterns and chromatic polarization patterns not only increases the dimension of information storage but also advances the security level of encryption.

Liquid crystal polymers (LCPs) are a class of ideal patterned polymer materials for constructing structural color patterns and chromatic polarization patterns, which possess the processability of polymers and the molecular anisotropy of liquid crystals.[21−26] On the one hand, the flowable precursors or prepolymers of LCPs provide the ability to be fabricated into precise micro/nanostructures by various methods, such as replica molding, colloidal lithography, and imprinting.[27,28] Subsequently, the micro/nanostructures are fixed by cross-linking occurring on the surface of LCPs films, enabling the creation of vibrant structural colors and intricate patterns. Yu et al. utilized the characteristic of azobenzene polymers to carry athermal transitions between different mechanical states under alternate lighting conditions, by which a multinanopattern was imprinted on flexible substrates using a mask template. This approach provided a way to prepare complex nanopatterns on the surface of polymer films, which were difficult to replicate and offered excellent encryption functionality.[29] On the other

Received: April 8, 2024
Revised: April 30, 2024
Accepted: May 6, 2024
Published: May 19, 2024

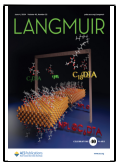

https://doi.org/10.1021/acs.langmuir.4c01297
Langmuir 2024, 40, 11766−11774

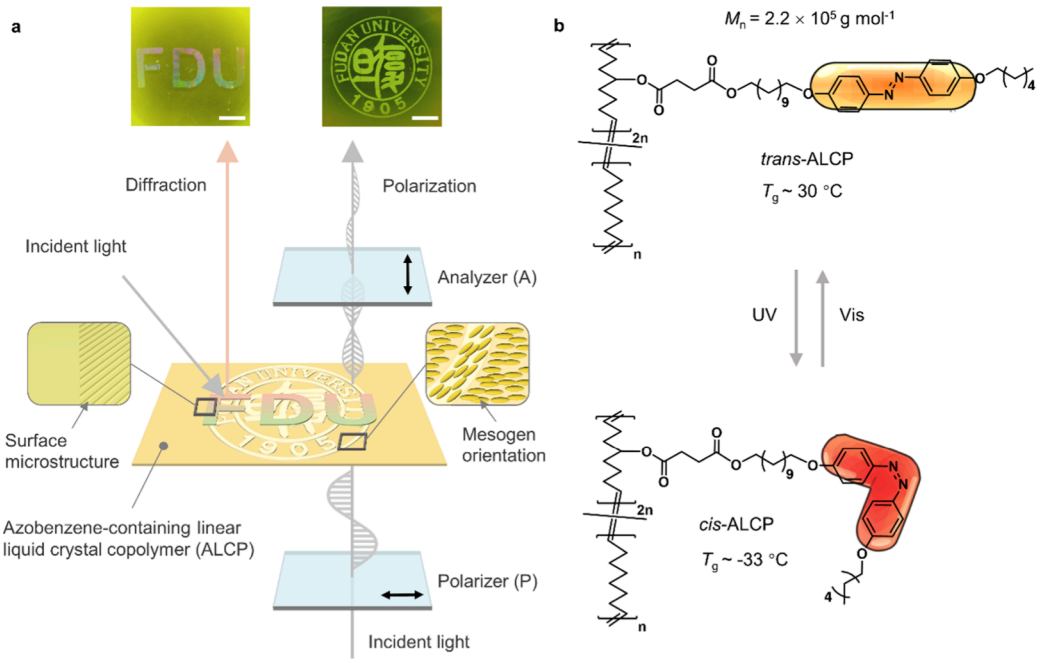

Figure 1. (a) Schematic and photographs of the azobenzene-containing linear liquid crystal copolymer (ALCP) films with dual-mode patterns observed in the reflection and polarization modes. The structural color patterns and chromatic polarization patterns come from the periodic microstructures and mesogens alignment, respectively. Scale bar: 5 mm. (b) Chemical structures and *trans*−*cis* photoisomerization of the ALCP. T_g, glass transition temperature; M_n, number-average molecular weight.

hand, a significant aspect of mesogens is their ability to control the polarization of light based on birefringence and optical anisotropy. Azobenzene is a versatile photoresponsive mesogen known for its ability to generate substantial structural and size changes via reversible *cis*−*trans* photoisomerization.[30−32] When incorporated into LCPs networks, the mesogens can be reorientated upon polarized light irradiation, known as the Weigert effect,[33−36] which imparts the ability of photopatterning based on chromatic polarization via precise local control. Wu et al. combined the photoresponsive properties of azobenzene liquid crystal polymers with upconversion nanoparticles to construct chromatic polarization patterns that exhibited high-contrast upconversion luminescent patterns under near-infrared light. Based on this, the combination of nanopattern imprinting and liquid crystal texture patterns was used to design four encryption patterns on banknotes.[37]

However, the introduction of two modes of patterns in the same location may lead to strong mutual interference during manufacturing and usage. First, traditional LCPs have physical or chemical cross-linked networks after the formation of micro/nanostructures, which restrict the photoreorientation of mesogens. Additionally, if micro/nanostructure embossing is conducted on the chromatic polarization patterns, localized deformation may possibly lead to changes in the orientation of mesogens and consequently affect the display of the chromatic polarization patterns. Therefore, independent storage and reading of these dual-mode patterns are significant challenges.

Herein, we report the preparation of noninterfering dual-mode patterns on a designed photofluidizable azobenzene-containing linear liquid crystal copolymer (ALCP). The glass transition temperature (T_g) of ALCP can be modulated by photofluidization, facilitating changes in both the mechanical characteristics of the polymer and the local orientation of the mesogens. Thanks to the linear structure of the ALCP, we can easily obtain structural color patterns by imprinting periodic micro/nanostructures through the photofluidization effect. In addition, photofluidization activates molecular segments and disrupts the physical cross-linking points formed by the self-assembly of *trans*-state azobenzene mesogens,[35,38−40] thereby promoting the photoreorientation for the preparation of chromatic polarization patterns. Hence, we propose a strategy for the sequential fabrication of these two patterns, enabling the creation of noninterfering dual-mode patterns in the same spatial location (Figure 1a). This approach significantly enhances the capabilities of polymers in terms of information storage and encryption.

EXPERIMENTAL SECTION

Materials. Azobenzene monomers and cyclooctene monomers were obtained according to the published articles.[35,39] The chemicals used in synthesis were all purchased from Sigma-Aldrich without further purification. The silicon template was purchased from Shanghai ZhiBan Electronic Science & Technology Co., Ltd.

Synthesis of the ALCP. The synthetic routes of the ALCP are described in Figure S1. The polymerization of ALCP was performed by using standard Schlenk techniques under a nitrogen atmosphere. The azobenzene monomer (1.354 g, 2 mmol) and cyclooctene monomer (0.132 g, 1.2 mmol) were added into a Schlenk flask. Then, 3 mmol of second-generation Grubbs catalyst with 3 mL of anhydrous dichloromethane was added to the mixture. After being stirred for 1 h at 50 °C, a yellow solid polymer was precipitated from methanol (1.332 g, 91%). All the results of ^{1}H NMR characterization are shown in Figure S2.

Measurements. *Cis*-ALCP was prepared following established protocols. The *trans*-ALCP was dissolved in CH_2Cl_2 and subsequently exposed to UV light at 365 nm and 100 mW cm^{-2} under stirring in the solution, and the solvent CH_2Cl_2 was then removed under vacuum conditions (7 mbar, 30 min) to generate a sufficient quantity of *cis*-ALCP for the subsequent measurements. The UV light source (UV-LED, Omron) is used for photofluidization. The controller type is ZUV-C30H, the illuminator type is ZUC-H30MC, the light source wavelength is 365 nm, and the light intensity can be adjusted in the

https://doi.org/10.1021/acs.langmuir.4c01297
Langmuir 2024, 40, 11766−11774

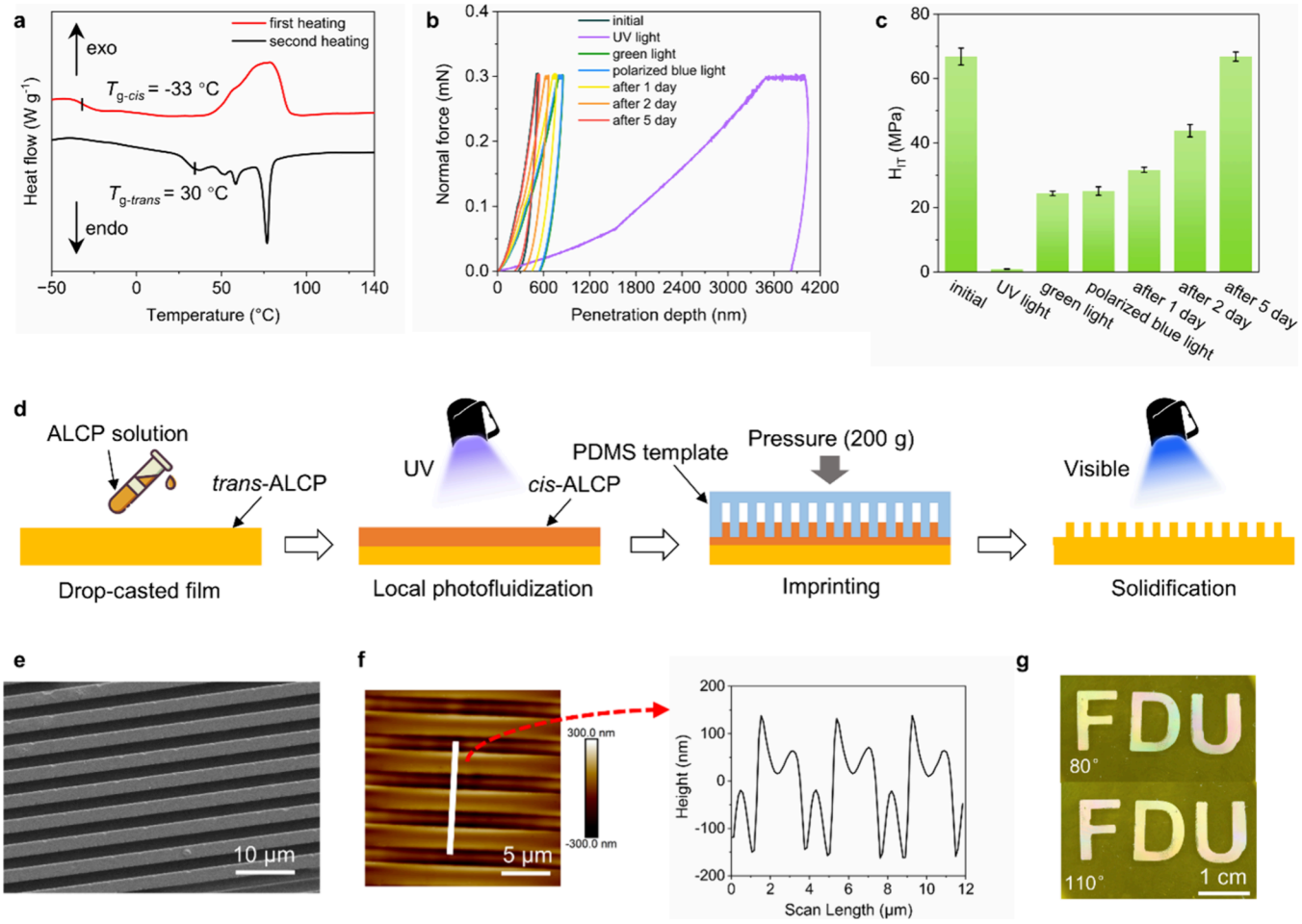

Figure 2. (a) Differential scanning calorimetry (DSC) curves of *trans*-ALCP and *cis*-ALCP. (b) Loading-pause-unloading displacement curves of the ALCP films in the initial state, after UV irradiation (365 nm, 100 mW cm^{-2}, 2 min), after green light irradiation (530 nm, 60 mW cm^{-2}, 10 min), after blue light irradiation (470 nm, 60 mW cm^{-2}, 10 min), and after several days. (c) A plot to compare the surface hardness of the ALCP films after different treatment. (d) Schematic diagram to show the fabrication process of structural color patterns by athermal microstructure imprinting. (e) SEM images to show the surface of the films imprinted with microstructures. (f) AFM images and height characterization of the films imprinted with microstructures. (g) Photographs of the films imprinted with the word "FDU" at different angles, which exhibit clear structural color patterns.

range of 0−160 mW cm^{-2}. The blue light source (LED, CCS, HLV-24BL-3W) was used for photoinduced orientation, and the wavelength is 470 nm. The green light source (LED, CCS, HLV-24GR-3W) is used for curing and reduction after photofluidization, and the wavelength is 530 nm. The light intensity can be adjusted in the range of 0−120 mW cm^{-2}. ^{1}H NMR spectra of the monomers and ALCP were recorded using a Bruker AVANCE III HD NMR spectrometer. Tetramethyl silane was employed as the internal standard, and $CDCl_3$ served as the solvent. The thermodynamic properties of both the obtained *trans*- and *cis*-ALCP were determined by using differential scanning calorimetry (DSC, TA, Q2000). The heating and cooling rates employed were set at 10 °C min^{-1}, within a temperature range of 60−150 °C. The photoisomerization of ALCP was characterized through ultraviolet and visible spectrophotometry (UV−Vis, PerkinElmer, Lambda 650). Fast scanning atomic force microscopy (AFM Bruker, Dimension FastScan) in the Tapping mode was used to characterize the size and depth of the microstructures. Scanning electron microscopy (FESEM, Zeiss, Ultra 55) was used to observe the surface morphology of the microstructure (sputtered with gold, accelerating voltage: 3 kV). A Canon camera (Canon, 70D) was used to shoot samples. The surface hardness of ALCP films was measured using an ultrananoindentation tester (CSM, UNHT) with a diamond intender. The indentation was carried out 9 times with the same test parameters, and the data obtained were averaged. Approach/retract speed: 2000 nm min^{-1}, max load: 0.30 mN, loading/unloading rate: 0.30 mN min^{-1}, and pause: 30.0 s. The experimental temperature was 25 °C.

Preparation of PDMS Template with Microstructure. The silicon template with a particular microstructure array was placed in the Petri dish, and an appropriate amount of PDMS prepolymer (mass ratio of monomer to cross-linkers was 10:1) was added. The Petri dish was then put into a vacuum drying oven and vacuumed at room temperature for 30 min until the air dissolved in the mixture was completely removed. The PDMS prepolymer was added carefully to completely cover the silicon template, and then a glass sheet was used to cover its top. After being heated in a 100 °C blast oven for 2 h, the PDMS template with a negative microstructure was formed and could be removed from the silicon template.

Preparation of ALCP Films. First, 30 mg of ALCP was dissolved in 1 mL of toluene, ensuring complete dissolution. The solution was filtered by using a syringe equipped with a needle-type filter. The filtered solution was slowly dropped onto a glass substrate measuring 3 cm × 4 cm. The glass substrate was placed on a hot plate at 50 °C to allow the toluene to evaporate and form a film. After solvent evaporation, the glass substrate with the film was transferred to an oven and annealed at 60 °C for 12 h. Following annealing, the ALCP film was carefully removed from the glass substrate. The resulting film had a thickness of approximately 20 μm.

Preparation of Structural Color Patterns. Ultraviolet light was shined and slit through a photomask onto the film (365 nm, 100 mW

https://doi.org/10.1021/acs.langmuir.4c01297
Langmuir 2024, 40, 11766−11774

cm^{-2}, 2 min). Next, a predesigned PDMS microstructure template was pressed onto the film (apply 200 g of weight), and this pressure was maintained for approximately 10 min. The mold was removed, and the film surface was irradiated with green light to revert it back to a relatively hard solid state (530 nm, 60 mW cm^{-2}, 2 min).

Preparation of Polarization Color Patterns. After 40 min of exposure to ultraviolet light (365 nm, 100 mW cm^{-2}), which fully fluidized the thin film, a 10 min exposure to polarized blue light (470 nm, 60 mW cm^{-2}) was performed to initiate the first photoreorientation. Following that, a hollow black PMMA mask was placed on the thin film, and another 20 min exposure to ultraviolet light (365 nm, 100 mW cm^{-2}) was performed to fluidize the hollowed areas, followed by a second photoreorientation using polarized blue light. The polarization direction of the polarized blue light used in both alignment processes had an angle of 45° between them.

Preparation of Dual-Mode Patterns. Exposure to ultraviolet light (365 nm, 100 mW cm^{-2}) for 40 min was performed to achieve full photofluidization of the ALCP films. Subsequently, a PMMA mask with Pattern 1 was applied to block light, preserving the *cis*-state in that specific area, while the remaining regions underwent simultaneous solidification and photo-orientation under polarized blue light (470 nm, 60 mW cm^{-2}). The mask was removed, and the shaded area was then subjected to imprinting using a PDMS microstructure template (2 μm linear microstructure template). Another round of ultraviolet light exposure was performed by using a mask with hollowed Pattern 2 to induce photofluidization in the region corresponding to Pattern 2. Then, the thin film was covered with a PMMA mask containing Pattern 1, effectively shielding the overlapping region of the two patterns. The remaining areas were subjected to photo-orientation under polarized blue light with a polarization direction of 45°. Subsequently, the mask was removed and the PDMS microstructure template was used for imprinting. Finally, the region that underwent imprinting was subjected to simultaneous photoreorientation and solidification under polarized blue light, resulting in the creation of a dual-mode pattern.

RESULTS AND DISCUSSION

Design and Synthesis of ALCP. Certain azobenzene-containing liquid crystal polymers have exhibited photofluidization, where they undergo a reversible transition from a solid (glassy state) to a liquid (highly elastic/viscous flow state) at room temperature when exposed to different wavelengths of light.[40−44] These polymers are noteworthy for their capacity to realize polymer alteration of mechanical properties and healing or reshaping at room temperature. To construct a dual-mode pattern combining structural color and chromatic polarization, we designed the photofluidizable ALCP based on three criteria: (1) the material is a linear structure and has considerable mechanical strength; (2) the material needs to undergo rapid and reversible mechanical state transitions under different lighting conditions; (3) the orientation of mesogens can be readjusted and fixed upon light irradiation.

The first requirement is satisfied by utilizing unique high-molecular-weight linear ALCP obtained through ring-opening metathesis polymerization (ROMP) to promote mechanical robustness, which was characterized by ^{1}H NMR and GPC (Figures 1b, S2, S3). To satisfy the second criterion, we devised a side-chain azobenzene group with a long alkyl tail, along with a flexible spacer positioned between the azobenzene group and the polycyclooctene backbone of ALCP. These structural modifications were intended to facilitate photo-induced reversible transition from the glassy to rubbery state. The glass transition temperature (T_g) of ALCP is initially higher than room temperature (about 30 °C), remaining in a glassy state with adequate mechanical strength and resistance to imprinting. After exposure to UV light, T_g decreases significantly to −33 °C, facilitating the transition into a rubbery state that can be easily imprinted (Figure 2a). To meet the third criterion, we conducted copolymerization of cyclooctene with azobenzene monomers in a molar ratio of 2:1, which was undertaken to introduce flexible alkyl chains into backbone for facilitating self-assembly of the mesogens. Additionally, it serves the purpose of concurrently lowering the side-chain density of the azobenzene mesogens, which increases the available free volume to promote the requisite *trans*−*cis*−*trans* isomerization cycle, thereby accelerating the process of photoreorientation.

Microstructure-Embossed Structural Color Patterns. The microstructure-embedded structural color patterns require materials for rapid and reversible mechanical state transitions under different lighting conditions. To confirm that the ALCP can be shaped and embossed after exposure to UV light, we investigated the photoswitchable mechanical properties of P1 by characterizing the surface hardness changes using nano-indentation after exposure to UV and visible light. As shown in the load-penetration depth curves (Figure 2b), the films after UV exposure (*cis*-state) exhibit an approximately 8-fold increase in penetration depth compared to the initial films and the films after exposure to visible light (*trans*-state). Moreover, during the load-holding stage, it shows a more pronounced creep behavior, which can be quantified by calculating the creep coefficient C of the sample,

$$C = \frac{D(\tau_L + \tau_H) - D(\tau_L)}{D(\tau_L)} \quad (1)$$

Where $D(\tau_L)$ and $D(\tau_L + \tau_H)$ represent the indentation depth at the end of the loading stage and the end of the equilibrium stage, respectively. Calculations show that the creep coefficients of the film are as follows: 0.045 (initial state), 0.145 (after UV exposure), 0.076 (after green light irradiation), and 0.082 (after polarized blue light irradiation). The increase in the creep coefficient and the significant change in penetration depth demonstrate that the surface hardness of the film can be rapidly switched through illumination. Combining the calculated surface hardness values, it can be concluded that UV light photofluidizes the film to an embossable state, while visible light solidifies the fluidized surface, turning it into an unembossable glassy state. Due to the presence of some *cis*-state azobenzenes in ALCP after visible light exposure, the surface hardness does not return to its initial state. We tested and found that after placing the polymer film at room temperature for 5 days, the surface hardness can recover to its initial state. Furthermore, both the load-penetration depth curves and surface hardness values indicate that using 530 nm green light and 470 nm polarized blue light achieves an equivalent curing effect. Therefore, there is no need for additional solidification with green light during the preparation of chromatic polarization patterns (Figure 2c).

Thanks to the macroscopic light-controlled reversible soft-to-hard transition of ALCP, it is possible to achieve localized embossing on the film surface with the aid of mask templates. As shown in Figure 2d, the ALCP film was prepared by drop-casting and then exposed to UV light through a photomask template (365 nm, 100 mW cm^{-2}, 2 min) to induce local *trans*−*cis* isomerization and solid-to-liquid transition. Then, a predesigned PDMS microstructure template (Figure S4) was pressed on the film to imprint (with a 200 g weight applied)

https://doi.org/10.1021/acs.langmuir.4c01297
Langmuir 2024, 40, 11766−11774

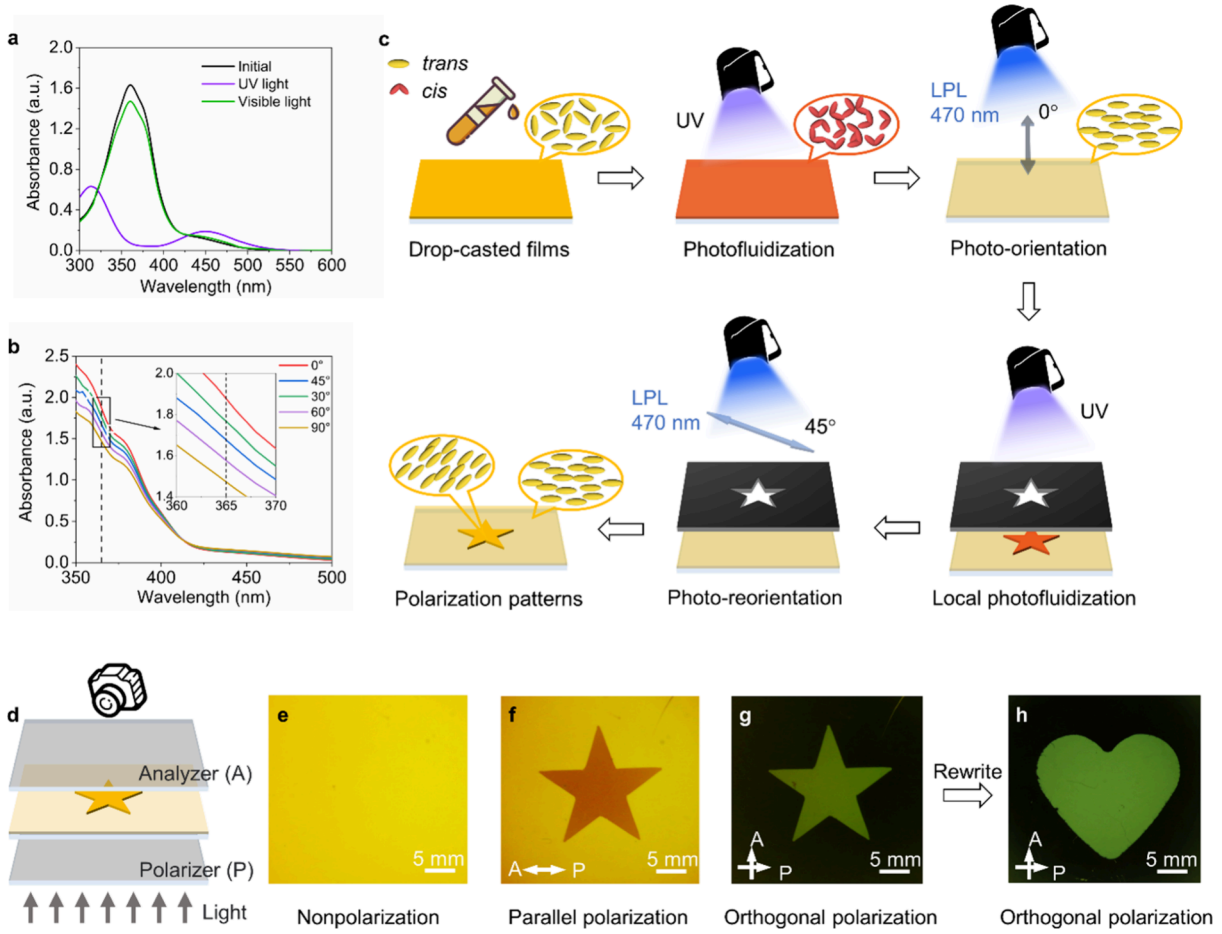

Figure 3. (a) Variation of the UV−Vis spectra of ALCP induced by UV and visible light irradiation. ALCP dissolved in CH_2Cl_2 solution (5×10^{-4} M). UV light: 365 nm, 20 mW cm^{-2}. Visible light: 530 nm, 20 mW cm^{-2}. (b) Polarized absorption spectra of the photo-oriented film after UV (365 nm, 100 mW cm^{-2}, 20 min) and linearly polarized blue light (470 nm, 60 mW cm^{-2}, 10 min) irradiation. (c) Schematic diagram to show the fabrication of the polarization-dependent pattern by photoreorientation. (d) Schematic diagram of the chromatic polarization patterns. Photographs of different polarized light: (e) without polarizer and analyzer; (f) polarizer parallel to analyzer; (g) polarizer orthogonal to analyzer. (h) Photograph to show the erasing and rewriting of the chromatic polarization patterns. The polarization directions for the crossed polarizers are P (polarizer) and A (analyzer).

for 10 min. After the template was removed, the film surface was irradiated with visible light to induce solidification (530 nm, 60 mW cm^{-2}, 2 min). This athermal process allows for the replication of periodic microstructure arrays onto the film surface and avoids the shrinkage from the thermal processing, thereby preserving the original pattern details to a great extent.

Through SEM and AFM characterization, it can be observed that the wide 2 μm linear microstructure is entirely intact with sharp edges, forming an ordered periodic arrangement that is well-organized and uniformly deep (Figure 2e−f). The periodic microstructure exhibits a colorful iridescent structural pattern when viewed under reflected light, resembling thin-film interference patterns (Figure 2g). The formation of this structural color pattern hinges on the periodic microstructure, and it can be erased and rewritten by photofluidizing the surface once again through UV light exposure (Figure S5).

Chromatic Polarization Patterns. Azobenzene mesogens exhibit unique photo-orientation properties based on the Weigert effect. When azobenzene molecules are irradiated with linearly polarized light (400−515 nm), those with a certain angle between their long axis and the polarization direction undergo a continual *trans*−*cis*−*trans* isomerization cycles until the long axis of the azobenzene molecules becomes perpendicular to the polarization direction of the light.[35,45,46] When azobenzenes are introduced into polymer networks, efficient photoreorientation is limited by the presence of physical or chemical cross-linking within the polymer networks. Therefore, we utilized the photofluidization of ALCP upon UV light irradiation, breaking the physical cross-linking and activating previously frozen molecular segments.[38−40] When fully photofluidized ALCP is irradiated with linearly polarized light, the reorientation of azobenzenes is no longer constrained by the polymer networks.

To demonstrate the feasibility of photoreorientation after photofluidization, we conducted polarized UV−Vis absorption tests. When the long axis of the azobenzenes forms different angles with the electric field vector of incident light (the polarization direction of linearly polarized light), the degree of photon energy absorption varies. Maximum absorption occurs when the long axis of the azobenzenes is parallel (0° or 180°) to the electric field vector of light, while minimal absorption occurs when it is perpendicular (90°), indicating almost no absorption of photon energy. Therefore, by changing the polarization direction of UV light, we can assess the photoreorientation results for thin films with respect to their absorption of UV light with different polarization directions.

https://doi.org/10.1021/acs.langmuir.4c01297
Langmuir 2024, 40, 11766−11774

According to the UV−Vis data of the ALCP solution, the $\pi-\pi^*$ absorption peak of the *trans*-azobenzene moieties is located at 365 nm (Figure 3a).

We tested their polarized UV−Vis absorption and analyzed the changes in the absorption intensity at 365 nm as we adjusted the polarization angle of the polarizer (Figure 3b). The angles marked in the figure represent the angle between the polarization direction of light and the direction of mesogen orientation. It can be observed that at an angle of 0°, the absorption at 365 nm is strongest. As the angle increases, the absorbance gradually decreases until it reaches a minimum at 90°. This indicates that the photofluidization followed by photoreorientation with polarized blue light has resulted in ALCP films with excellent mesogen orientation.

To obtain chromatic polarization patterns, it is necessary to achieve a uniform orientation within the thin films. In other words, polymer films with full photofluidization are required, and UV light exposure time is an important factor in this process. Due to the high absorbance of azobenzene, during short-term UV light exposure, only the surface azobenzenes undergo *trans*−*cis* isomerization. As the exposure time increases, the surface azobenzenes transform into the *cis* state with low-absorbance UV light so that the deeper azobenzenes can be excited. It should be noted that during exposure to polarized blue light, the azobenzene groups undergo *trans*−*cis*−*trans* isomerization cycles. When a significant portion of the *cis*-state azobenzene transforms into the *trans* state, the T_g of the films increases above room temperature, and the azobenzenes become less able to freely reorient. Thus, increasing the exposure time to polarized blue light is dispensable.

We prepared uniform ALCP films (approximately 15 μm) by using a drop-casting method. These films were then cut into several rectangles of the same size and subjected to different durations of UV light exposure (365 nm, 100 mW cm^{-2}). Subsequently, they were exposed to polarized blue light for 10 min (470 nm and 60 mW cm^{-2}). The degree of orientation was determined by polarized optical microscopy (POM) images taken at different angles (Figure S6). When UV light was not applied and only polarized blue light was performed, the azobenzene mesogens within the films exhibited multiple domains and showed opacity because of frozen molecular segments. As the UV light exposure time increased, the film became gradually more transparent due to the enhanced orientation, leading to significant differences in brightness in the POM images. As shown in Figure S6, it can be inferred that photoreorientation is almost finished when the UV light exposure time exceeds 20 min.

After determining the duration of UV light exposure, we used a mask to prepare ALCP films with different local orientations. Based on the birefringence phenomenon of mesogens, regions with different orientations under polarized light exhibited brightness differences, allowing construction of chromatic polarization patterns. As shown in Figure 3c, we initially prepared drop-casting with a thickness of approximately 15 μm and then exposed to UV light for 40 min (365 nm, 100 mW cm^{-2}) to complete photofluidization. Subsequently, the films were exposed to 0° polarized blue light (470 nm, 60 mW cm^{-2}) for 10 min to achieve the first photo-orientation, resulting in a monodomain orientation. Next, we placed a "star-shaped" black PMMA mask on the films and exposed it to another UV light exposure for 20 min (365 nm, 100 mW cm^{-2}) to photofluidize the "star-shaped" region. A second round of photo-orientation was performed with 45° polarized blue light to make the orientation different from the other regions. It is important to note that the duration of UV light exposure affects the degree of orientation of the films, further influencing transparency. Therefore, we controlled the duration of UV light exposure for the first orientation to be longer than that for the second, ensuring that the films reached a high level of transparency after the first alignment. This prevented significant differences in transparency between the two regions, which could impact the encrypted storage of the chromatic polarization patterns.

We explored the transmission patterns under different illumination modes (Figure 3d). Observing the resulting films under nonpolarized light, the color appeared uniform and the chromatic polarization patterns were not visible, allowing for information hiding and encryption (Figure 3e). Due to the 45° angle difference in the mesogen orientation between the "star-shaped" region and the background, when observed between two parallel polaroids, there was a difference in brightness between these areas, enabling the visualization of chromatic polarization patterns (Figure 3f). This effect is achieved through the birefringence phenomenon of liquid crystals: when the liquid crystal orientation matches the polarization direction of linearly polarized light, the polarized light can fully pass through. However, when the mesogen orientation is at a 45° angle with respect to the polarization direction of the light, half of the refracted light is filtered by the analyzer, resulting in reduced brightness. The differences in brightness between regions with different orientations under linearly polarized light allow chromatic polarization patterns to be displayed, facilitating a convenient information reading. When the film was observed under orthogonal polarization (i.e., with the polarizer and analyzer perpendicular to each other), the orientation of the background region was kept parallel to either the polarizer or analyzer to appear black. Meanwhile, the orientation of the "star-shaped" region held 45° to both the polarizer and analyzer caused it appear bright (Figure 3g). In summary, through the method of thorough photofluidization followed by photoreorientation, we obtained chromatic polarization patterns that are invisible under nonpolarized light but visible with high contrast under polarized light.

Since thorough UV photofluidization was performed before photoreorientation, erasing and rewriting chromatic polarization patterns is very convenient. We subjected the film with the photo-oriented "star-shaped" pattern to full UV photofluidization once again and performed photoreorientation as described before, resulting in a "heart-shaped" pattern (Figures 3h, S7)

Noninterfering Dual-Mode Patterns. We have successfully prepared two single-mode patterns: structural color patterns generated through microstructure imprinting and chromatic polarization patterns created through photoreorientation. The challenge in constructing dual-mode patterns arises from the fact that when writing the second pattern in the same location, the microstructure and molecular arrangement of the first pattern could be easily disturbed, leading to pattern destruction. In this work, we encountered a similar issue: structural color patterns are derived from microstructures and can be erased due to molecular chain movement during subsequent UV exposure, while chromatic polarization patterns heavily rely on the alignment of liquid crystals, which can be disrupted by UV exposure and microstructure construction. To

https://doi.org/10.1021/acs.langmuir.4c01297
Langmuir 2024, 40, 11766−11774

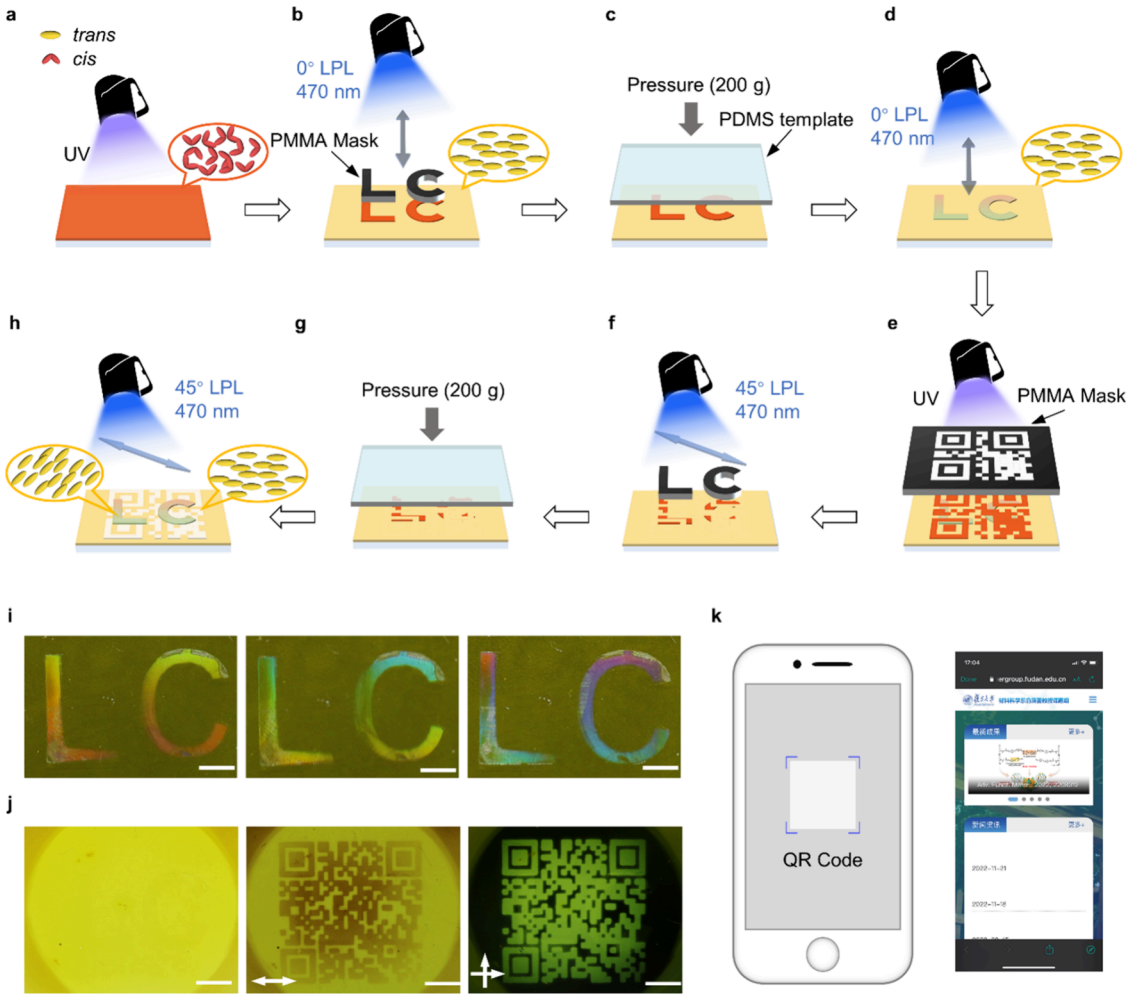

Figure 4. Preparation process of dual-mode patterns. (a) Photofluidization of the film by UV illumination, with the red region indicating the *cis*-ALCP. (b) Coverage of the "LC" area by a PMMA mask, with the yellow area indicating the *trans*-ALCP, which is photo-oriented by 0° linear polarized blue light. (c) Removal of the PMMA mask and imprinting of only the red *cis* region by the PDMS templates. (d) Simultaneous orientation and curing of the "LC" region by 0° linear polarized blue light, with the gradient color indicating the surface microstructure region. (e) Photofluidization of the "QR code" region by UV illumination through the mask. (f) Coverage of the "LC" area by a PMMA mask, with the rest of the area photo-oriented by 45° linear polarized blue light. (g) Removal of the PMMA mask and imprinting of only the red *cis* region by the PDMS templates. (h) Simultaneous orientation and curing of the "LC" region by polarized blue light, resulting in the successful creation of a dual-mode pattern. (i) Photographs to show the structural color patterns with imprinted microstructure. Scale bar: 5 mm. (j) Photographs showing the chromatic polarization patterns with a high-resolution "QR code". Scale bar: 5 mm. (k) Schematic illustration showing the decryption of the chromatic polarization "QR code" pattern.

address this challenge, we propose a strategy for simultaneously creating both patterns. We took advantage of UV exposure to ensure thorough photofluidization of the film. Then, we simultaneously created both patterns and used polarized blue light to solidify the microstructures from the imprinting process and achieve the reorientation of mesogens. This results in the creation of dual-mode patterns that do not interfere with each other. Previous experiments have confirmed that polarized blue light can achieve the same solidification effect as green light, making it a necessary condition for simultaneously creating two patterns. This approach allows us to achieve the coexistence of two distinct patterns without compromising their integrity, offering a solution to the challenges associated with constructing dual-mode patterns in the same location.

The steps to create the dual-mode pattern (Figure 4a–h) are as follows: (a) Exposure to ultraviolet light (365 nm, 100 mW cm^{-2}) for 40 min to fully photofluidize the films, containing a significant amount of *cis*-state azobenzenes. (b) Cover the area with the word "LC" using a PMMA mask, leaving the "LC" area predominantly in the *cis* state. Subsequently, use 0° linear polarized blue light for photo-orientation. The light-yellow area represents the *trans* state and horizontal orientation. (c) Remove the mask and use a PDMS microstructure template (2 μm line pattern template) for imprinting. Only the red "LC" area can be imprinted. (d) Simultaneously, orient and solidify the "LC" area using 0° linear polarized blue light. The gradient color area represents the structural color pattern from microstructure imprinting. (e) Use a mask for ultraviolet light exposure to photofluidize the "QR code" area. (f) Cover the area with the word "LC" using a PMMA mask. At this point, only the overlapping area between the "LC" and the "QR code" is preserved. Then, use 45° linear polarized blue light for photoreorientation. (g) Remove the mask and use a PDMS microstructure template for imprinting. Only the red *cis*-state area can be imprinted. (h) Simultaneously, align and

https://doi.org/10.1021/acs.langmuir.4c01297
Langmuir 2024, 40, 11766−11774

solidify the imprinted area using 45° linear polarized blue light, resulting in the dual-mode pattern. Two important points to note are that the "LC" area (the imprinting area) is covered and preserved during the photoreorientation process using a mask. The imprinting process only alters the surface microstructure, and the orientation within the structure is still obtained by polarized blue light. The ability of polarized blue light to simultaneously orient and solidify the ALCP films is a crucial prerequisite for this method. The reason for the second imprinting of "LC" is that polarized-related patterns require two different local liquid crystal alignments, necessitating a two-step process to create both patterns simultaneously.

The obtained dual-mode pattern can be read separately under different lighting conditions without interference: Under nonpolarized transmitted light, the dual-mode patterns are not visible (Figure 4i). When nonpolarized light is incident at a certain angle that satisfies the Bragg diffraction condition, the imprinted microstructure exhibits a colorful structural "LC" pattern, containing 29 × 29 pixels in 2 cm × 2 cm areas (Figure 4j). Thanks to the high precision of light, we utilized high-resolution QR code patterns easily to achieve the storage and encryption of web page information (Figure 4k). Furthermore, high-molecular-weight polymer materials can self-support and adhere to everyday goods, which can be recognized by using polarized light sources such as liquid crystal displays, making them highly valuable for practical applications.

CONCLUSION

We have demonstrated the preparation of dual-mode patterns using ALCP via photofluidization with subsequent imprinting and photoreorientation. On the one hand, we realized the fabrication of structural color patterns using microstructure imprinting based on the switchable mechanical states. On the other hand, we utilized the photoreorientation to construct chromatic polarization patterns thanks to the improvement of the azobenzene motion ability after photofluidization. Based on the preparation principles of these two single-mode patterns, we proposed a strategy for simultaneously fabricating dual-mode patterns at the same location without interference, thereby enabling independent identification of the two patterns. Furthermore, due to the absence of chemical cross-linking in ALCP, these dual-mode patterns can be easily erased and rewritten through photofluidization. The information storage characteristics ingrained in these dual-mode pattern labels manifest outstanding resolution, enduring durability, and rapid recognition via the naked eye, delivering an innovative strategy for the creation of advanced encryption technology.

ASSOCIATED CONTENT

Supporting Information

The Supporting Information is available free of charge at https://pubs.acs.org/doi/10.1021/acs.langmuir.4c01297.

Chemical structures, synthesis routes, experimental characterizations, and photo images (PDF)

AUTHOR INFORMATION

Corresponding Authors

Lang Qin − *Department of Materials Science and State Key Laboratory of Molecular Engineering of Polymers, Fudan University, Shanghai 200433, China;* orcid.org/0000-0002-7439-225X; Email: qinlang@fudan.edu.cn

Yanlei Yu − *Department of Materials Science and State Key Laboratory of Molecular Engineering of Polymers, Fudan University, Shanghai 200433, China;* orcid.org/0000-0002-4623-3331; Email: ylyu@fudan.edu.cn

Authors

Feng Pan − *Department of Materials Science and State Key Laboratory of Molecular Engineering of Polymers, Fudan University, Shanghai 200433, China*

Yaoqing Feng − *Department of Materials Science and State Key Laboratory of Molecular Engineering of Polymers, Fudan University, Shanghai 200433, China*

Yuyao Qian − *Department of Materials Science and State Key Laboratory of Molecular Engineering of Polymers, Fudan University, Shanghai 200433, China*

Complete contact information is available at: https://pubs.acs.org/10.1021/acs.langmuir.4c01297

Notes

The authors declare no competing financial interest.

ACKNOWLEDGMENTS

This work was financially supported by the National Natural Science Foundation of China (52233001, 51927805) and the Innovation Program of Shanghai Municipal Education Commission (2023ZKZD07).

REFERENCES

(1) Kragt, A. J. J.; Hoekstra, D. C.; Stallinga, S.; Broer, D. J.; Schenning, A. P. H. J. 3D Helix Engineering in Chiral Photonic Materials. *Adv. Mater.* **2019**, *31*, 1903120.

(2) Qin, L.; Liu, X.; He, K.; Yu, G.; Yuan, H.; Xu, M.; Li, F.; Yu, Y. Geminate Labels Programmed by Two-Tone Microdroplets Combining Structural and Fluorescent Color. *Nat. Commun.* **2021**, *12*, 699.

(3) Jeon, J.; Bukharina, D.; Kim, M.; Kang, S.; Kim, J.; Zhang, Y.; Tsukruk, V. Tunable and Responsive Photonic Bio-Inspired Materials and Their Applications. *Responsive Mater.* **2024**, *2*, No. e20230032.

(4) Lin, X.; Shi, D.; Yi, G.; Yu, D. Structural Color-Based Physical Unclonable Function. *Responsive Mater.* **2024**, *2*, No. e20230031.

(5) Feng, J.; Yang, F.; Wang, X.; Lyu, F.; Li, Z.; Yin, Y. Self-Aligned Anisotropic Plasmonic Nanostructures. *Adv. Mater.* **2019**, *31*, 1900789.

(6) Zhou, X.; Wang, L.; Wei, Z.; Weng, G.; He, J. An Adaptable Tough Elastomer with Moisture-Triggered Switchable Mechanical and Fluorescent Properties. *Adv. Funct. Mater.* **2019**, *29*, 1903543.

(7) Dietrich, M.; Delaittre, G.; Blinco, J. P.; Inglis, A. J.; Bruns, M.; Barner-Kowollik, C. Photoclickable Surfaces for Profluorescent Covalent Polymer Coatings. *Adv. Funct. Mater.* **2012**, *22*, 304−312.

(8) Huang, L.; Wu, W.; Li, Y.; Huang, K.; Zeng, L.; Lin, W.; Han, G. Highly Effective Near-Infrared Activating Triplet-Triplet Annihilation Upconversion for Photoredox Catalysis. *J. Am. Chem. Soc.* **2020**, *142*, 18460−18470.

(9) Lin, S.; Tang, Y.; Kang, W.; Bisoyi, H. K.; Guo, J.; Li, Q. Photo-Triggered Full-Color Circularly Polarized Luminescence Based on Photonic Capsules for Multilevel Information Encryption. *Nat. Commun.* **2023**, *14*, 3005.

(10) Heuser, T.; Merindol, R.; Loescher, S.; Klaus, A.; Walther, A. Photonic Devices Out of Equilibrium: Transient Memory, Signal Propagation, and Sensing. *Adv. Mater.* **2017**, *29*, 1606842.

(11) Farrukh, A.; Paez, J. I.; del Campo, A. 4D Biomaterials for Light-Guided Angiogenesis. *Adv. Funct. Mater.* **2019**, *29*, 1807734.

(12) Kim, S.-U.; Lee, Y.-J.; Liu, J.; Kim, D. S.; Wang, H.; Yang, S. Broadband and Pixelated Camouflage in Inflating Chiral Nematic Liquid Crystalline Elastomers. *Nat. Mater.* **2022**, *21*, 41−46.

(13) Pelloth, J. L.; Tran, P. A.; Walther, A.; Goldmann, A. S.; Frisch, H.; Truong, V. X.; Barner-Kowollik, C. Wavelength-Selective Softening of Hydrogel Networks. *Adv. Mater.* **2021**, *33*, 2102184.
(14) Cui, S.; Qin, L.; Liu, X.; Yu, Y. Programmable Coloration and Patterning on Reconfigurable Chiral Photonic Paper. *Adv. Opt. Mater.* **2022**, *10*, 2102108.
(15) Zhang, M.; Pal, A.; Zheng, Z.; Gardi, G.; Yildiz, E.; Sitti, M. Hydrogel Muscles Powering Reconfigurable Micro-Metastructures with Wide-Spectrum Programmability. *Nat. Mater.* **2023**, *22*, 1243−1252.
(16) Liu, X.; Cui, S.; Qin, L.; Yu, Y. Two-Chromatic Printing Creates Skin-Inspired Geminate Patterns Featuring Crosstalk-Free Chemical and Physical Colors. *Adv. Opt. Mater.* **2024**, *12* (12), 2302573.
(17) Nie, Z.; Kumacheva, E. Patterning Surfaces with Functional Polymers. *Nat. Mater.* **2008**, *7*, 277−290.
(18) Xiang, L.; Li, Q.; Li, C.; Yang, Q.; Xu, F.; Mai, Y. Block Copolymer Self-Assembly Directed Synthesis of Porous Materials with Ordered Bicontinuous Structures and Their Potential Applications. *Adv. Mater.* **2023**, *35*, 2207684.
(19) Chen, S.; Ma, T.; Bai, J.; Ma, X.; Yin, J.; Jiang, X. Photodynamic Pattern Memory Surfaces with Responsive Wrinkled and Fluorescent Patterns. *Adv. Sci.* **2020**, *7*, 2002372.
(20) Deng, S.; Huang, L.; Wu, J.; Pan, P.; Zhao, Q.; Xie, T. Bioinspired Dual-Mode Temporal Communication via Digitally Programmable Phase-Change Materials. *Adv. Mater.* **2021**, *33*, 2008119.
(21) de Gennes, P.-G. One Type of Nematic Polymers. *Comptes Rendus Hebd. Seances Acad. Sci. Ser. B* **1975**, *281*, 101−103.
(22) Finkelmann, H.; Kock, H.-J.; Rehage, G. Liquid-Crystalline Elastomers - A New Type of Liquid-Crystalline Material. *Makromol. Chem., Rapid Commun.* **1981**, *2*, 317−322.
(23) Gao, J.; Tian, M.; He, Y.; Yi, H.; Guo, J. Multidimensional-Encryption in Emissive Liquid Crystal Elastomers through Synergistic Usage of Photorewritable Fluorescent Patterning and Reconfigurable 3D Shaping. *Adv. Funct. Mater.* **2022**, *32*, 2107145.
(24) Yi, H.; Gao, J.; Lin, S.; Ma, J.; Guo, J. Photoresponsive α-Cyanostilbene-Containing Fluorescent Liquid Crystal Polymers Based on Ring-Opening Metathesis Polymerization for Information Storage and Encryption. *Polymer* **2022**, *258*, 125289.
(25) Ji, Y.; Song, T.; Yu, H. Assembly-Induced Dynamic Structural Color in a Host-Guest System for Time-Dependent Anticounterfeiting and Double-Lock Encryption. *Angew. Chem., Int. Ed.* **2024**, No. e202401208.
(26) Wang, H.-Q.; Tang, Y.; Huang, Z.-Y.; Wang, F.-Z.; Qiu, P.-F.; Zhang, X.; Li, C.-H.; Li, Q. A Dual-Responsive Liquid Crystal Elastomer for Multi-Level Encryption and Transient Information Display. *Angew. Chem., Int. Ed.* **2023**, *62*, No. e202313728.
(27) Zhang, P.; de Haan, L. T.; Debije, M. G.; Schenning, A. P. H. J. Liquid Crystal-Based Structural Color Actuators. *Light-Sci. Appl.* **2022**, *11*, 248.
(28) Foelen, Y.; Schenning, A. P. H. J. Optical Indicators Based on Structural Colored Polymers. *Adv. Sci.* **2022**, *9*, 2200399.
(29) Yang, B.; Cai, F.; Huang, S.; Yu, H. Athermal and Soft Multi-Nanopatterning of Azopolymers: Phototunable Mechanical Properties. *Angew. Chem., Int. Ed.* **2020**, *59*, 4035−4042.
(30) Kumar, G. S.; Neckers, D. C. Photochemistry of Azobenzene-Containing Polymers. *Chem. Rev.* **1989**, *89*, 1915−1925.
(31) White, T. J.; Broer, D. J. Programmable and Adaptive Mechanics with Liquid Crystal Polymer Networks and Elastomers. *Nat. Mater.* **2015**, *14*, 1087−1098.
(32) Finkelmann, H.; Nishikawa, E.; Pereira, G. G.; Warner, M. A New Opto-Mechanical Effect in Solids. *Phys. Rev. Lett.* **2001**, *87*, 015501.
(33) Weigert, F. Uber Einen Neuen Effekt der Strahlung in Lichtempfindlichen Schichten. *Verh. Dtsch. Phys. Ges.* **1919**, *21*, 479−491.
(34) Yu, Y.; Nakano, M.; Ikeda, T. Directed Bending of a Polymer Film by Light. *Nature* **2003**, *425*, 145.
(35) Lv, J.; Liu, Y.; Wei, J.; Chen, E.; Qin, L.; Yu, Y. Photocontrol of Fluid Slugs in Liquid Crystal Polymer Microactuators. *Nature* **2016**, *537*, 179−184.
(36) Pang, X.; Lv, J.; Zhu, C.; Qin, L.; Yu, Y. Photodeformable Azobenzene-Containing Liquid Crystal Polymers and Soft Actuators. *Adv. Mater.* **2019**, *31*, 1904224.
(37) Xu, W.; Liu, C.; Liang, S.; Zhang, D.; Liu, Y.; Wu, S. Designing Rewritable Dual-Mode Patterns Using a Stretchable Photoresponsive Polymer via Orthogonal Photopatterning. *Adv. Mater.* **2022**, *34*, 2202150.
(38) Pang, X.; Qin, L.; Xu, B.; Liu, Q.; Yu, Y. Ultralarge Contraction Directed by Light-Driven Unlocking of Prestored Strain Energy in Linear Liquid Crystal Polymer Fibers. *Adv. Funct. Mater.* **2020**, *30*, 2002451.
(39) Feng, Y.; Wei, J.; Qin, L.; Yu, Y. Three-Dimensional Liquid Crystal Polymer Actuators Assembled by Athermal Photo-Welding. *Soft Matter* **2023**, *19*, 999−1007.
(40) Xu, B.; Zhu, C.; Qin, L.; Wei, J.; Yu, Y. Light-Directed Liquid Manipulation in Flexible Bilayer Microtubes. *Small* **2019**, *15*, 1901847.
(41) Baroncini, M.; d'Agostino, S.; Bergamini, G.; Ceroni, P.; Comotti, A.; Sozzani, P.; Bassanetti, I.; Grepioni, F.; Hernandez, T. M.; Silvi, S.; Venturi, M.; Credi, A. Photoinduced Reversible Switching of Porosity in Molecular Crystals Based on Star-Shaped Azobenzene Tetramers. *Nat. Chem.* **2015**, *7*, 634−640.
(42) Zhou, H.; Xue, C.; Weis, P.; Suzuki, Y.; Huang, S.; Koynov, K.; Auernhammer, G. K.; Berger, R.; Butt, H. J.; Wu, S. Photoswitching of Glass Transition Temperatures of Azobenzene-Containing Polymers Induces Reversible Solid-to-Liquid Transitions. *Nat. Chem.* **2017**, *9*, 145−151.
(43) Xu, W.; Sun, S.; Wu, S. Photoinduced Reversible Solid-to-Liquid Transitions for Photoswitchable Materials. *Angew. Chem., Int. Ed.* **2019**, *58*, 9712−9740.
(44) Chen, M.; Yao, B.; Kappl, M.; Liu, S.; Yuan, J.; Berger, R.; Zhang, F.; Butt, H.; Liu, Y.; Wu, S. Entangled Azobenzene-Containing Polymers with Photoinduced Reversible Solid-to-Liquid Transitions for Healable and Reprocessable Photoactuators. *Adv. Funct. Mater.* **2020**, *30*, 1906752.
(45) Natansohn, A.; Rochon, P. Photoinduced Motions in Azo-Containing Polymers. *Chem. Rev.* **2002**, *102*, 4139−4176.
(46) Qin, L.; Liu, X.; Yu, Y. Soft Actuators of Liquid Crystal Polymers Fueled by Light from Ultraviolet to Near Infrared. *Adv. Opt. Mater.* **2021**, *9*, 2001743.

https://doi.org/10.1021/acs.langmuir.4c01297
Langmuir 2024, 40, 11766−11774